PROGRESS IN PHOTOVOLTAICS: RESEARCH AND APPLICATIONS
Prog. Photovolt: Res. Appl. 2007; **15**:303–315
DOI: 10.1002/pip.739

Research

Experimental Solar Spectral Irradiance Until 2500 nm: Results and Influence on the PV Conversion of Different Materials

J. J. Pérez-López*,†, F. Fabero and F. Chenlo
CIEMAT—DER, Laboratorio de Componentes y Sistemas Fotovoltaicos, Avda. Complutense, 22. 28040 Madrid, Spain

In this work, results are presented concerning solar spectral irradiance measurements performed in Madrid in the wavelength range 250–2500 nm, that is, extending the spectral range far away from the wavelengths where PV semiconductors are active. These data were obtained considering a horizontal receiver surface during selected clear days covering the four seasons of the year. PV materials having different spectral responses (m-Si, a-Si, CIGS, CdTe) have been considered to calculate spectral factors (SF) taking as reference the standard solar spectrum AM1.5 defined in standard IEC 60904-3. From these SFs, the influence of natural solar spectral variations in PV conversion has been established. It is shown, for example, that PV technologies based on a-Si are highly favored, from the spectral point of view, in spring–summer compared to other technologies having broader spectral responses, which are more favored in autumn–winter. From the experimental measured solar spectra, we have calculated Weighed Solar Spectra (WSS) corresponding to the four seasons of the year and also to the whole year. The WSS represents, for a certain period of time, the solar spectrum weighed over the irradiance level. SFs have been calculated for different WSSs showing spectral gains for the four PV materials during almost the full year. Otherwise, it is also shown in this work how the near-IR part of the solar spectrum affects the evaluation of the solar resource as a whole when reference solar cells made of different PV materials are used. For typical m-Si, a-Si, CIGS, and CdTe solar cells, the ratio of I_{sc} over global irradiance is not constant along a given day showing variations that depend on the season and on the PV material considered. © 2006 John Wiley & Sons, Ltd.

KEY WORDS: solar spectral irradiance; mismatch calculation; spectral response; reference cell

Received 1 June 2006; Revised 6 October 2006

---

* Correspondence to: J. J. Pérez-López, CIEMAT, Department of Energy, Photovoltaic Energy Division, Avda. Complutense, n° 22. 28040 Madrid, Spain.
†E-mail: jjpl0001@estudiante.ujaen.es

INTRODUCTION

Nowadays, an extensive worldwide database containing data for horizontal global solar irradiance is available. Many stations record global, direct, diffuse solar irradiance, and other meteorological parameters allowing to the development of some series of sufficiently checked models that are extremely useful to evaluate the components of solar irradiance on plane ground. However, the spectral distribution of the solar irradiance and its dependence on geographical, astronomical, and atmospheric factors has not been sufficiently addressed yet. The knowledge of this term is important for the estimation of yearly energy productions of systems that, using solar radiation as a source of energy, are spectrally selective like, for example, all those based in photovoltaic conversion.

Several attempts have been made to estimate the effect of solar spectral variations in PV conversion. For example in Reference1 Hirata *et al*. make use of a six-band spectroradiometer to calculate the ratio of spectral solar radiation available for solar cell (p-Si and a-Si) utilization to global solar radiation. After 1 year of measurements, they compared the experimental $P_{\max}$ output of several modules with the theoretical prediction obtaining accurate results relative to spectral effects. Results could be improved by increasing the resolution of the spectroradiometer used. Other authors, like Betts *et al*.,[2,3] make use of a parameter called average photon energy (APE) to account for spectral effects. This magnitude relates the energy of a given solar spectrum with the relative optical air mass AM and the clearness index K_T. The disadvantage of APE is that it does not allow a direct determination of the spectral effect on a PV device. For this reason, the authors define a useful fraction UF of irradiance by means of the ratio of the integrated spectral irradiance within the response band of a given PV material to the total irradiance, thus considering flat spectral responses in the calculation of UF. Good correlations between APE and UF were obtained.

The key parameter to be used in the study of the influence of the solar spectral irradiance in PV conversion is the short-circuit current (I_{sc}), defined as:

$$I_{sc} = A \int_{\lambda} E(\lambda) \cdot SRa(\lambda) \cdot d\lambda$$

where A is the total area of the PV device, $SRa(\lambda)$ its absolute spectral response, and $E(\lambda)$ is the solar spectral irradiance. I_{sc} is influenced by any change in the solar spectral distribution that takes place in the wavelength range where the PV material is active. In this work, we have studied such an influence by means of the so-called a Spectral Factor (*SF*)[4] or Mismatch Factor (MMF),[5] that can be defined as:

$$\mathrm{SF} = \frac{\int E_{\mathrm{STD}}(\lambda) \cdot SRr(\lambda) \cdot d\lambda / \int E_{\mathrm{STD}}(\lambda) \cdot d\lambda}{\int E_{\mathrm{EXP}}(\lambda) \cdot SRr(\lambda) \cdot d\lambda / \int E_{\mathrm{EXP}}(\lambda) \cdot d\lambda}$$

where:

- $E_{\mathrm{STD}}(\lambda)$ is the reference solar spectral distribution defined in the standard IEC 60904-3,[6]
- $SRr(\lambda)$ is the relative spectral response of the PV device considered,
- $E_{\mathrm{EXP}}(\lambda)$ is the actual measured solar spectrum.

From the definition of *SF*, it results that a value of *SF* higher than 1 means that the actual solar spectral distribution is producing in the PV material considered a short-circuit current that is, taking spectral issues only into account, lower than the I_{sc} obtained under the reference solar spectral distribution. Otherwise, a value of *SF* lower than 1 means that there is a gain in the short-circuit current (with the consequence of a greater power and greater performance) compared to the I_{sc} under the standard solar spectrum IEC 60904-3. When considering the production of energy with PV materials, it is very clear that spectral effects will be of greater importance at high irradiance levels, when the solar resource is large. For this reason, it is convenient to define[7] a Weighed Solar

DOI: 10.1002/pip

Spectrum (WSS) as:

$$\mathrm{WSS}(\lambda) = \frac{\sum_{i=1}^{i=n} E_i(\lambda) \cdot \left(\int_{\lambda} E_i(\lambda)\mathrm{d}\lambda\right)}{\sum_{i=1}^{i=n} \left(\int_{\lambda} E_i(\lambda)\mathrm{d}\lambda\right)}$$

being:

- $E_i(\lambda)$ is solar spectral irradiance at a given time,
- n is the total number of different solar spectra considered to be weighed.

WSS(λ) so defined represents, for a certain period of time, the solar spectrum under which PV materials are producing energy weighed over the irradiance level. Consequently, if we calculate WSS(λ) for a full clear day, then the most influencing solar spectra in the calculation will be those corresponding to times near noon. Considering WSS(λ) for a full year the solar spectra in summer should be the most influencing part in the total calculation. WSS(λ)s can be used to get a close approach of the spectral conditions most prevailing at a given place in energy rating calculations.

In this work, we present a daily and yearly study of the evolution of *SF*s corresponding to four different PV materials. We have considered several types of solar spectra to perform the calculations: experimental solar spectra and several calculated WSSs (seasonal and annual). Results included in this work overcome some of the limitations of previous papers because we are using experimental solar spectra (measured in the 250–2500 nm wavelength region having 1 nm resolution) and real relative spectral responses that we consider representative of four different semiconductor materials that have PV modules commercially available nowadays, that is, m-Si, a-Si (single junction), CIGS, and CdTe, as shown in Figure 1. The different distribution in wavelengths of these spectral responses is very suitable for the purposes of this work because they are centered in different parts of the solar spectrum and are also different in wide. Data from Figure 1 have not been measured in this work but obtained from previous published results.[8,9]

The use of *SF*s to calculate solar spectral influences on the conversion efficiency of a-Si and m-Si PV devices has been previously reported in Reference 4 also considering the direct and diffuse components of the sunlight in Reference 7. However, all these works were based on solar spectral measurements in the 300–1100 nm

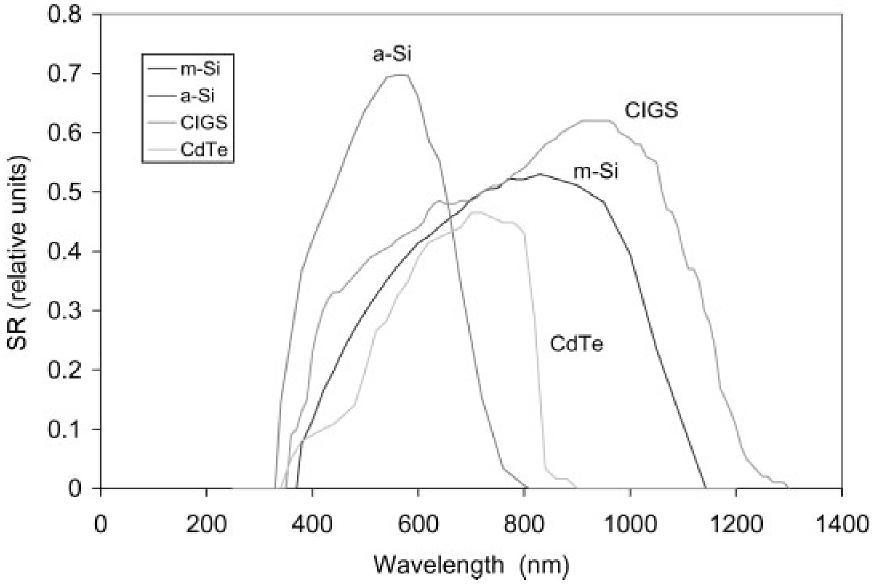

Figure 1. Relative spectral responses of the different PV materials considered in this work

DOI: 10.1002/pip

wavelength range. In this work, we extend far away in the infrared the wavelength range in which the calculations are performed, according to the relative spectral responses of the PV materials considered in Figure 1 and to the actual sunlight resource.

The importance of solar spectral variations issues in indoor and outdoor calibration or measurements of PV solar devices has been pointed out by several authors.[10–13] Natural solar spectral variation effects can be particularly important when comparing the differential performance of different PV technologies under real operation. In this work, we have compared the I_{sc} produced by typical m-Si, a-Si (single junction), CIGS, and CdTe solar cells (based on calculations from the relative spectral responses included in Figure 1) with the corresponding integrated experimental solar irradiance (250–2500 nm). Daily non-linear relationships between both magnitudes have been found that should be related only to spectral issues because our results are based in calculations and not in real measurements of I_{sc}s. Real measurements are affected by other factors such as, for example, temperature and angular effects that are not considered in this paper.

EXPERIMENTAL

To perform solar spectral radiation measurements, we have used a spectroradiometer MONOLIGHT™ model 6602 whose measurement range is 250–2500 nm. A view of this spectroradiometer can be found in Figure 2. The resolution used during measurements is 1 nm and the scan time for the whole range of wavelengths ranges between 100 and 300 s (typically 120 s), depending on the intensity of the sunlight to be measured. The optical receptor of the spectroradiometer consists in an integrating sphere (6 inches diameter) having a hemispherical quartz dome (3·5 inches diameter). The input port of sunlight to the integrating sphere is a circular hole having a diameter of 2·2 inches located under the quartz dome. The sphere is internally covered with Labsphere Spectralon®, a nearly constant 100% reflective material in the wavelength range of interest. A set of internal baffles prevents input light from reaching directly the input port to the spectroradiometer body. The monochromator system is made of two holographic gratings that are mounted in a moving platform that is rotating at a speed of 1 turn per second. This system would allow to scan the full range of wavelengths every second but to increase the signal-to-noise ratio several turns are needed, depending on the intensity and stability of the sunlight to be measured, as stated above. The detectors, located at the exit slit of the monochromator, are

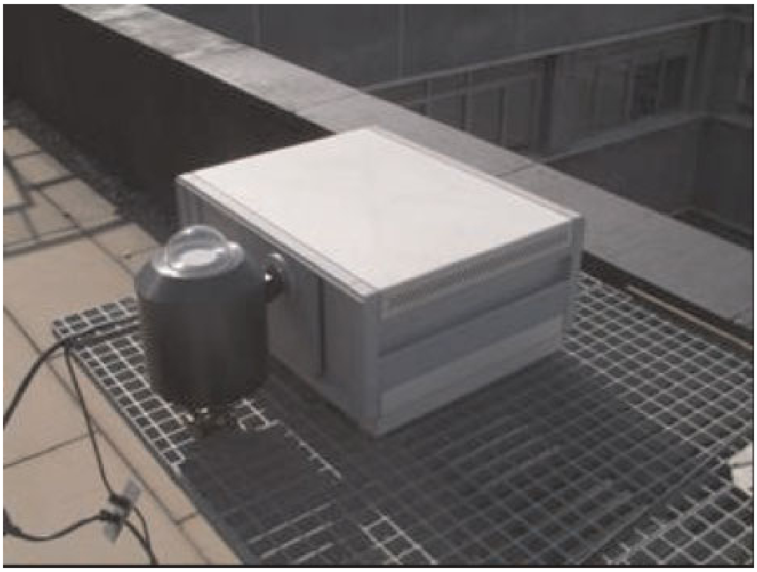

Figure 2. General view of the spectroradiometer used in this work showing the quartz dome and the weatherproof enclosure of the integrating sphere

DOI: 10.1002/pip

Si (for 250–1095 nm wavelength range) and InGaAs (for the 1095–2500 nm wavelength range) photodiodes. To minimize temperature effects, both detectors are thermoelectrically cooled. All measurements were taken on the roof of the building of the Renewable Energy Department of CIEMAT in Madrid (40·45°N, 3·73°W, 620 m above sea level). Solar spectra were measured only in selected clear days (no visible clouds), covering the four seasons of the year considering a horizontal receiver plane. Delay time between consecutive spectra during the measuring days was 30 min. The spectroradiometer was periodically calibrated using a reference lamp traceable to NPL (National Physics Laboratory, UK). The spectral irradiance of the calibration lamp together with the Standard Solar Spectrum IEC 60904-3 are included in Figure 3. It can be seen in this Figure that the calibration lamp shows enough light intensities at all the wavelengths of interest for the intended use of the spectroradiometer. Measurement results concerning the cosine response of the integrating sphere show a deviation lower that 10% from the cosine law at incident angles higher than 45°.

Integrated global (horizontal) irradiance was measured at the same time of the recording of the solar spectra by an Eppley PSP pyranometer and a data-logger HP-Agilent.

Linearity of the spectroradiometric measurements can be a problem considering the type of spectral measurements that are presented in this paper, with very different sunlight intensities that are measured with two different detectors. We have investigated linearity in two ways. On one hand, we have used the calibration lamp as light source considering different light intensities at the input port of the integrating sphere. The different intensities were obtained not by changing the current feeding the lamp (that would modify the lamp spectrum) but by rotating the integrating sphere through the axis that joins the sphere with the main body of the spectroradiometer (see Figure 2 where it can be seen that this type of rotation is easily allowed). The measured spectra are included in Figure 4 (0° corresponds to perpendicular incidence of the light beam relative to the plane that contains the input port). Relative linearity of both detectors was checked by comparing in each spectrum the integrals of the different portions measured by the detectors (250–1095 nm and 1095–2500 nm respectively).

The ratio of the different integrals is included in Table I (integral values in relative arbitrary units).

It is only at 75° when the difference of ratios compared to 0° is higher than 2%, mainly because of the noisy part of the spectrum above 2200 whose magnitude is almost equal at all light intensities. The relative linearity of both detectors seems to be reasonably fine at the different light intensities considered in the calibration lamp.

On the other hand, linearity has been checked by comparing the integral (between 250 and 2500 nm, i.e., full range) of the solar spectral irradiance measured by the spectroradiometer with the integrated global (horizontal)

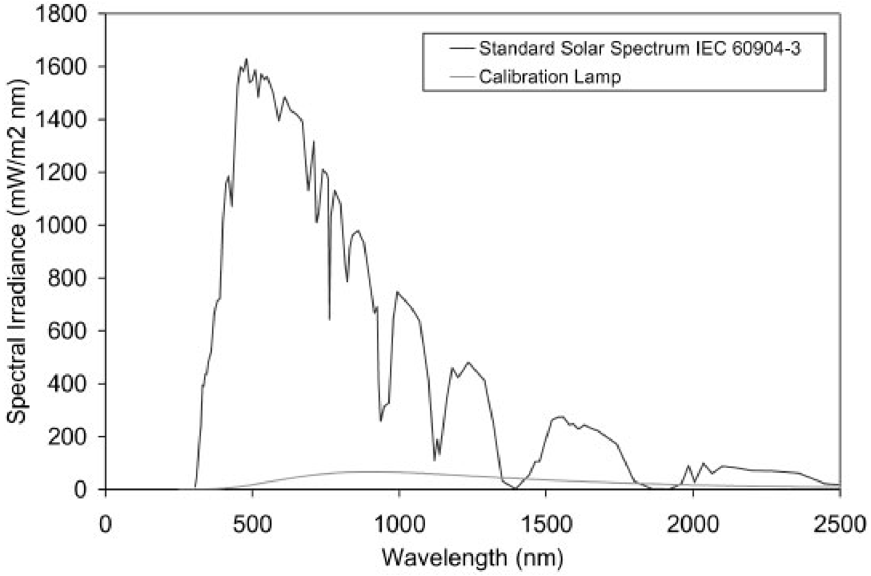

Figure 3. Spectral irradiance of the calibration lamp of the spectroradiometer. IEC 60904-3 Standard Solar Spectrum is also included for comparison purposes of relative intensities

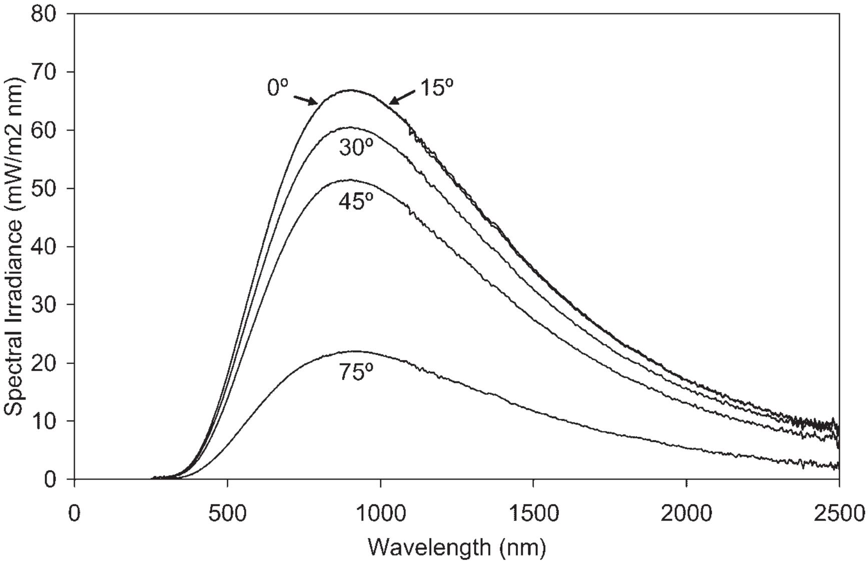

Figure 4. Calibration lamp spectra at different rotation angles of the integrating sphere of the spectroradiometer

irradiance measured with the pyranometer described above. In Figure 5, we show the result obtained for a representative clear spring day (26 May 2003).

Assuming that the pyranometer signal is linear with solar irradiance, it seems to be clear that the spectroradiometer shows the same behavior as the pyranometer. Differences observed in late afternoon can be assigned to several factors (different IR content of the solar spectrum compared to the morning, temperature effects associated to the pyranometer signal, different angular behavior between both instruments because of the low solar elevation, etc.). In any case, results of SFs presented in the paper mainly cover the solar time range between 08:24 and 15:36, that is, 0·35 and 0·65 in decimal format, where the signals form the pyranometer and from the spectroradiometer are practically superimposed.

RESULTS

Figures 6–9 show the daily evolution of the *SF*s calculated from solar spectra measured in different clear days (winter, spring, summer, and autumn) for the four PV materials considered in this work. Results corresponding to a total of 6 clear days are included in these Figures. Solar time is expressed in decimal format. Because nice weather conditions are "not selectable," we can include in this work only results obtained during days where measurements were allowed, always trying to include representative days covering the full year. In our study, we have performed solar spectrum measurements only in clear days only for several reasons. On one hand, clear days are the best days for PV module performance evaluation and calibration. The target of this paper is mainly

Table I. Calculation of the relative linearity of the detectors of the spectroradiometer used in this work

Angle of rotation	Integral (250–1095)	Integral (1095–2500)	Ratio
0°	33 763	38 468	0·8777
15°	33 763	38 158	0·8848
30°	30 556	34 842	0·8770
45°	26 010	29 264	0·8888
75°	11 071	12 307	0·8996

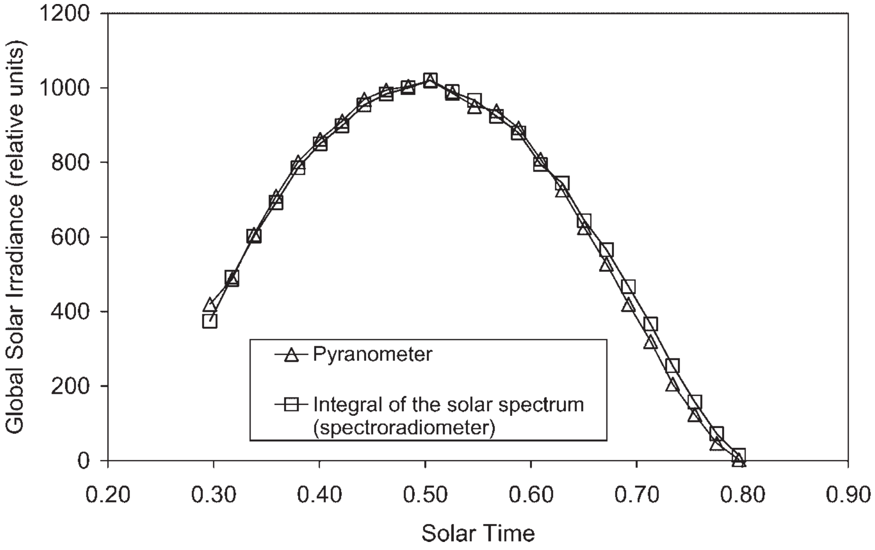

Figure 5. Comparison of the integrated solar irradiance measured by the spectroradiometer and by the pyranometer on a typical clear spring day (26-May-2003)

focused in these fields. On the other hand, cloudy days usually show large irradiance variations in short periods of time that make difficult to obtain solar spectra at stable irradiance conditions. Some examples of sharp irradiance variations during cloudy days in our measuring site can be found in Reference 14. It should be taken in mind that our spectroradiometer lasts around 2 min to perform a full solar spectrum. Finally, clear days are representative of the most prevailing conditions in our measuring site.[14]

Only results obtained at high irradiance time periods (8:30 to 15:30 solar time) are included in Figures 6–9. The spectral responses of the materials are quite different (see Figure 1) resulting in different *SF*s for each technology: the narrower the spectral response, the more sensitive the *SF* is. Technologies based in a-Si or CdTe are highly favored, from the spectral point of view, in spring–summer compared to other technologies like m-Si or CIGS, that are favored in winter.

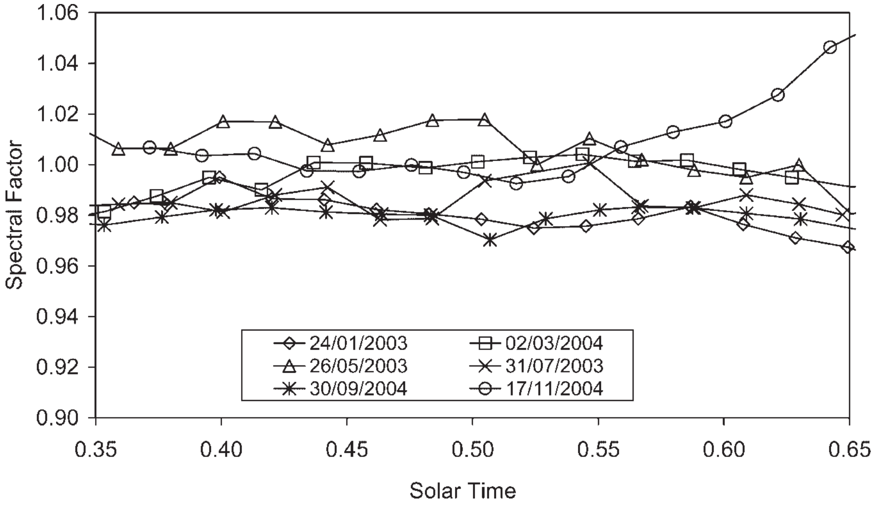

Figure 6. *SF*s for m-Si in different clear days

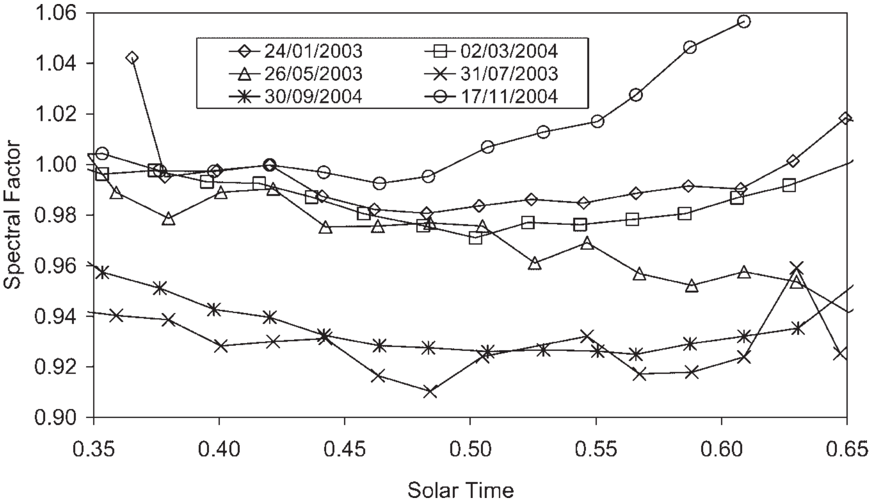

Figure 7. *SF*s for a-Si in different clear days

Spectral gains in I_{sc} for a-Si and CdTe are very large in some seasons. For example, the gain in summer can be near 8% for a-Si and 5% for CdTe, compared to gains of around 2% and 1% for m-Si and CIGS respectively. Considering winter the situation is not as different as in summer: all the four materials show spectral gains of around 2%. It is mainly in spring when some losses in I_{sc} can be found in m-Si and CIGS. In autumn, the gains in CdTe and a-Si can be around 6% and in m-Si and CIGS can be around 2.5%. In Figure 10, we present a detail of Figures 6–9 considering only noon, that is, the most sunny part in clear days. We can see in Figure 10 that, considering a whole year, a-Si is the most sensitive material to solar spectral variations, as expected from its narrow spectral response. For m-Si and CIGS, having a relative wide spectral response, there are some spectral losses in spring–early summer. In autumn and winter, all four materials have spectral gains. The largest spectral gains correspond to a-Si and CdTe. Otherwise, the less sensitive materials to spectral changes are m-Si and CIGS whose *SF*s lie in the range ±3% at noon during the full year.

To study spectral effects based on WSS, we have calculated four (one per season) WSS for Madrid obtained from measurements taken at 24 January 2003 (Winter), 2 March 2004 (considered as Spring), 31 July 2003 (Summer), and 17 November 2004 (Autumn). We include results in Figure 11.

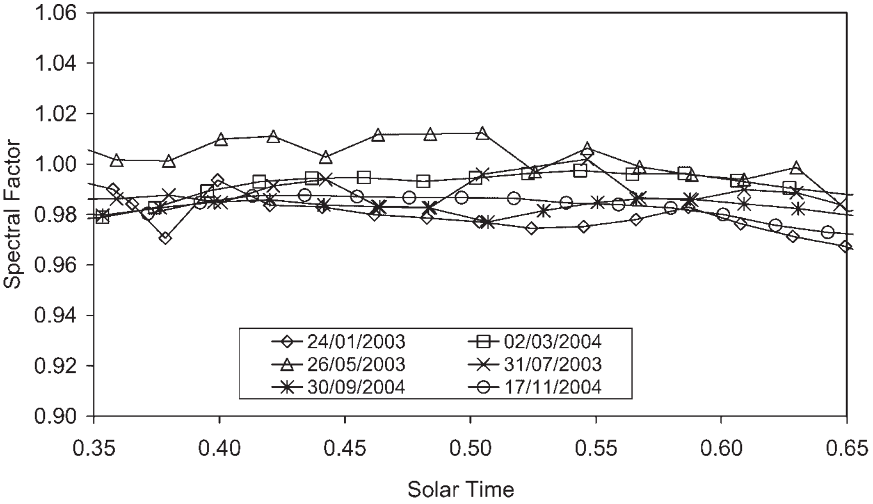

Figure 8. *SF*s for CIGS in different clear days

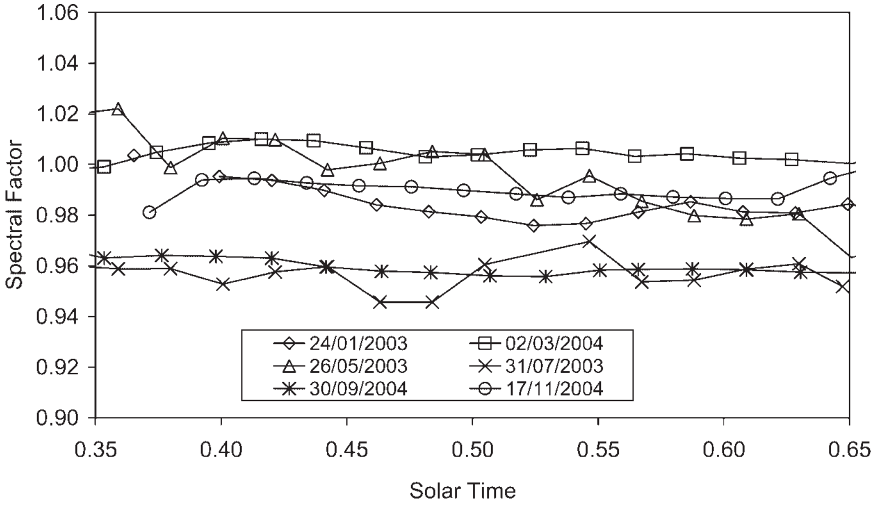

Figure 9. *SF*s for CdTe in different clear days

In this Figure, the spectra are plotted without any normalization, that is, these spectra have been obtained directly from the experimental measured spectra. We also include what we have called in this Figure ''Yearly WSS'' that has been calculated considering all the measurements taken during the four measuring days. As we can see in Figure 11, the spectra corresponding to winter and autumn seem to be very similar in intensity and relative spectral content. Otherwise, the Yearly WSS is very close to the WSS corresponding to spring. Summer is obviously, the season where the solar resource is higher in Madrid. It should be taken into account that only clear days are included in our study for the reasons stated above. Although the number of days used to calculate WSS(λ) is rather small (one per season), we think that they are representative enough to study the seasonal differential behavior of the four PV materials considered.

We have calculated the *SF*s corresponding to the spectra included in Figure 11. They are plotted in Figure 12. Results indicate that spectral gains (i.e., *SF* lower than 1) are obtained practically for all seasons and materials, mainly for a-Si and CdTe. Considering, a yearly basis the energy produced by the four PV materials considered

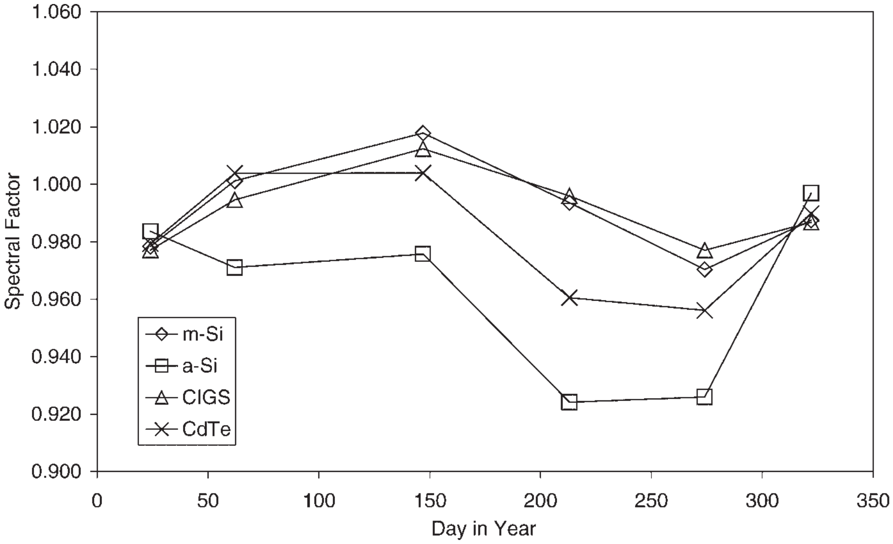

Figure 10. *SF*s at noon (clear days) for different PV materials

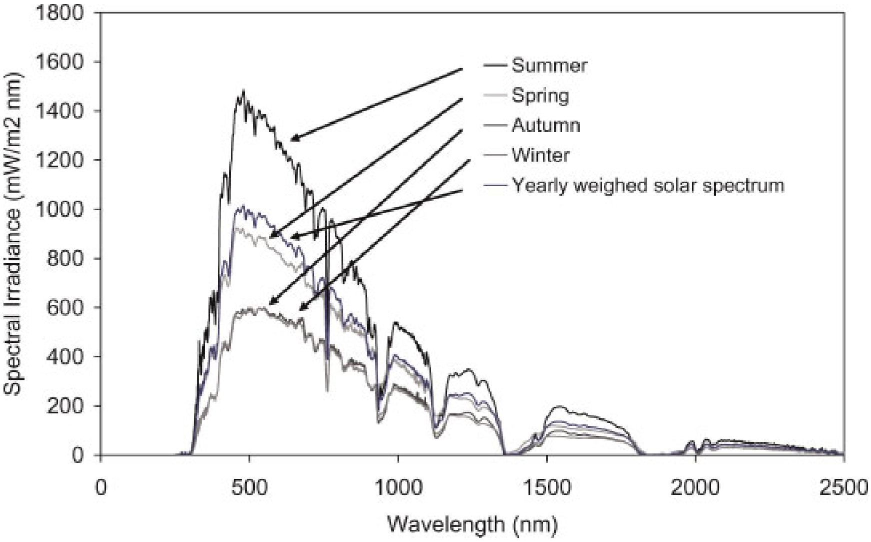

Figure 11. Experimental Absolute WSS (only clear days)

in this work is generally more favored by the actual solar spectrum (at high irradiance levels) than by the standard spectrum IEC 60904-3. Obviously, Figures 10 and 12 are quite similar as noon is usually the most sunny period of the day. Our results are in agreement with results obtained by other authors[15,16] that compare the different performance of PV materials (amorphous silicon, CIS, CdTe, crystalline silicon technologies) in real installations at two locations: thin-film technologies show higher performance than conventional crystalline silicon technologies. In these works, the authors conclude that not only spectral effects (also associated to cloud cover) but also thermal effects are responsible for this effect. In our work, that only considers spectral effects on clear days (and no thermal effects), we show that the same conclusions hold.

Results presented in this work can be interesting to study, for example, spectral issues associated to the calibration of reference solar cells, that are used many times to monitor solar irradiance in large PV plants. In Figures 13 and 14, we show the daily evolution during two different days (winter and summer typical clear days)

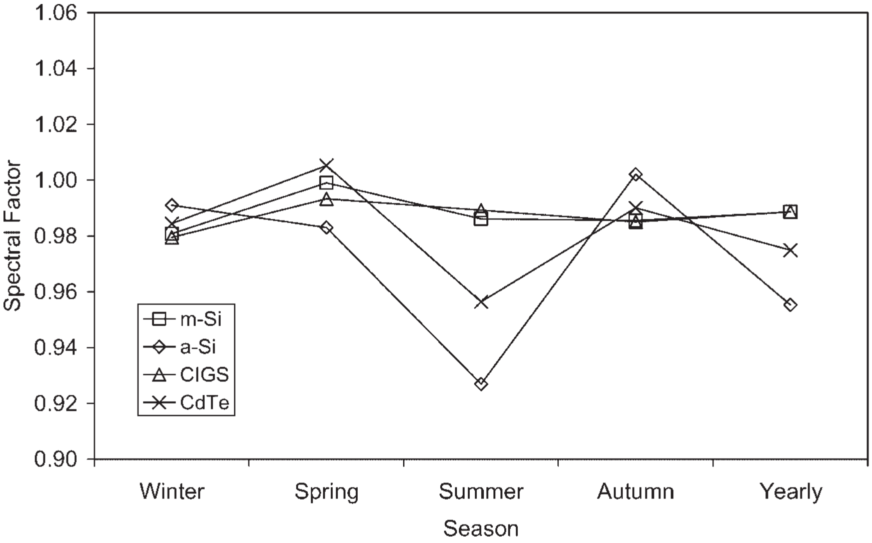

Figure 12. *SF*s calculated with WSS(λ) for different PV materials

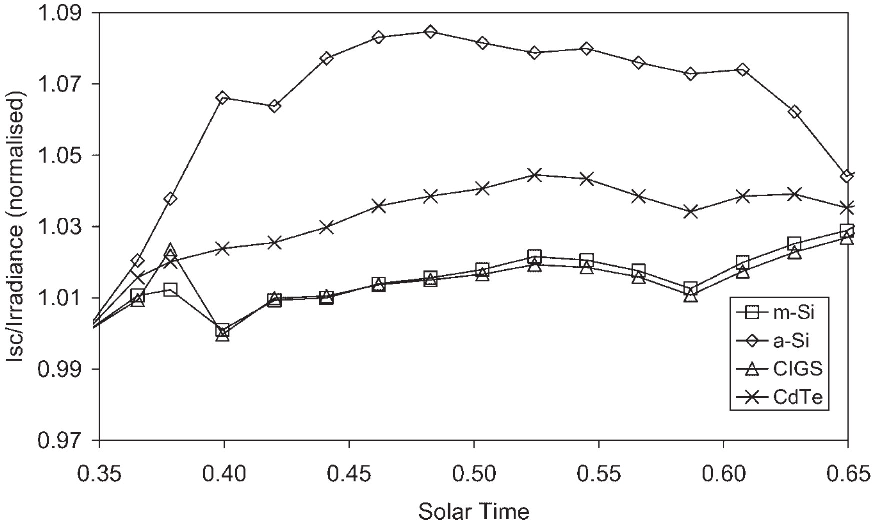

Figure 13. Ratio "I_{sc}"/Irradiance versus solar time for a typical clear winter day (24-Jan-2003)

of the ratio of "I_{sc}" (calculated by integrating the product $SRr(\lambda) \cdot E_{EXP}(\lambda)$, with $SRr(\lambda)$ included in Figure 1) over the integrated global solar spectral irradiance (calculated as the integral of $E_{EXP}(\lambda)$) for the four materials considered. As stated above, we are not considering other parameters influencing the measurement of solar radiation with solar cells as for example temperature or angular effects. Result included in Figures 13–14 show that the ratio varies along the day in all seasons, that is, I_{sc} is not fully linear with the integrated irradiance during a given day because of spectral effects. Furthermore, there are remarkable differences depending on the season of the year and on the PV material considered. The point above can be easily understood, if we consider that most of the IR part of the solar spectrum is not seen by PV solar cells, resulting in inaccuracies to estimate integrated irradiance when the solar spectrum is red-shifted, as it happens in autumn–winter and during extreme sunshine hours. When calculating the performance of a PV module, the total solar resource should be taken into account, and not only that part that can be converted to electricity by the module. In Table II, a summary of the maxima differences observed in the ratios included in Figures 13 and 14 is presented.

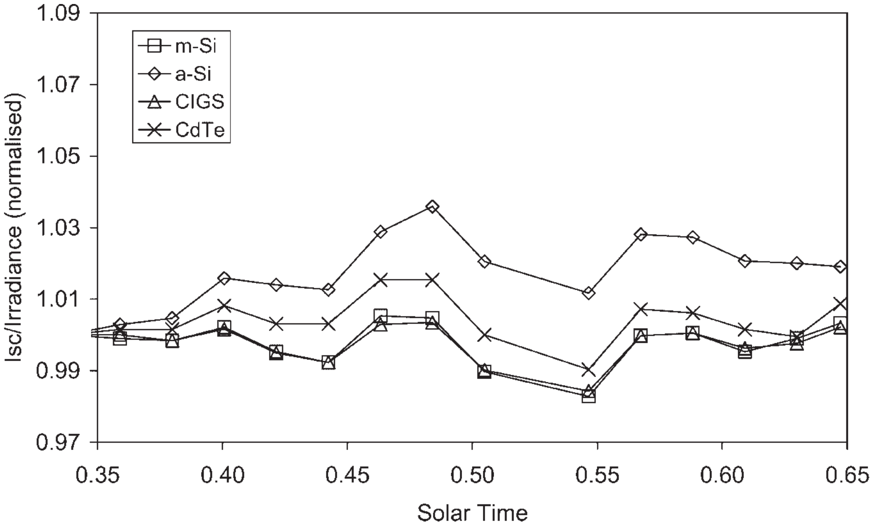

Figure 14. Ratio "I_{sc}"/Irradiance versus solar time for a typical clear summer day (31-Jul-2003)

Copyright © 2006 John Wiley & Sons, Ltd.

Table II. Maxima differences (%) obtained in the ratio "I_{sc}"/Irradiance

	Winter (24-Jan-2003)	Summer (31-Jul-2003)
m-Si	2·89	1·72
a-Si	8·47	3·59
CIGS	2·36	1·57
CdTe	4·45	1·53

Results in Table II indicate that, considering a full day, the non-linearity is higher in winter than in summer for all the four PV materials, that is, during this season, the natural solar spectral variations are larger for a given day. Considering the different materials, a-Si shows the maximum non-linearity.

CONCLUSIONS

PV conversion efficiency of semiconductors has been shown to be a seasonal dependent issue because of natural solar spectrum variations: some materials are much more favored for operation in summer time (a-Si, CdTe) than in winter time (m-Si, CIGS). PV materials having narrow spectral responses (a-Si, CdTe) are much more sensitive to spectral effects than other PV materials with wide spectral responses (m-Si, CIGS). WSS have been presented in this work corresponding to the four seasons of the year and also to the full year. Calculations of SFs using these Weighed Spectra lead to the conclusion that, in general, all PV materials considered in this work are more or less favored for producing energy on a yearly basis due to spectral effects, but at a different extent. Special care should be taken when using PV solar cells for monitoring solar irradiance: natural solar spectral variations cause a non-linearity of I_{sc} versus integrated global irradiance that can lead to some errors if spectral corrections are not made.

Acknowledgements

One of the authors (J. J. Pérez-López) greatly acknowledges CIEMAT for an FPI grant, and the necessary supplies to carry out this research.

REFERENCES

1. Hirata Y, Tany T. Output variation of photovoltaic modules with environmental factors-I. The effect of spectral solar radiation on photovoltaic module output. *Solar Energy* 1995; **55**(6): 463–468.
2. Betts TR, Gottschalg R, Infield DG. Spectral irradiance correction for PV system yield calculation. *Proceedings of the 19th European PVSEC*, Paris, 2004; 2533–2536.
3. Betts TR, Jardine CN, Gottschalg R, Infield DG, Lane K. Impact of spectral effects on the electrical parameters of multijunction amorphous silicon cells. *Proceedings of the 3rd World Conference in PV Energy Conversion*, Osaka, 2003; 1756–1759.
4. Fabero F, Vela N, Chenlo F. Influence of solar spectral variations on the conversion efficiency of a-Si and m-Si PV Devices: A yearly and hourly study. *Proceedings of the 13th European PVSEC*, Nice, 1995; 2281–2284.
5. Müllejans H, Ioannides A, Kenny R, Zaaiman W, Ossenbrink H, Dunlop E. Spectral mismatch in calibration of photovoltaic reference devices by global sunlight method. *Measurement Science and Technology* 2005; **16**: 1250–1254.
6. International Electrotechnical Commission. Standard IEC 60904-3: Photovoltaic Devices. Part 3: Measurement Principles for Terrestrial Photovoltaic (PV) Solar Devices with Reference Spectral Irradiance Data. 1989.
7. Fabero F, Chenlo F. Variance in the solar spectrum with the position of the receiver surface during the day for PV applications. *Proceedings of the 22nd IEEE PVSC*, Las Vegas, 1991; 812–817.
8. Mueller RL. The calculated influence of atmospheric conditions on solar cell I_{sc} under direct and global solar irradiances. *Proceedings of the 19th IEEE PVSC*, New Orleans, 1987; 166–170.

9. Field H. Solar cell spectral response measurement errors related to spectral band width and chopped light waveform. *Proceedings of the 26th IEEE PVSC*, Anaheim, 1997; 471–474.
10. Metzdorf J, Winter S, Wittchen T. Radiometry in photovoltaics: calibration of reference solar cells and evaluation of reference values. *Metrologia* 2000; **37**(5): 573–578.
11. Knaupp W. Power rating of photovoltaic modules from outdoor measurements. *Proceedings of the 22nd IEEE PVSC*, Las Vegas, 1991; 620–624.
12. Marion B. A method for modelling the current-voltage curve of a PV module for outdoor conditions. *Progress in Photovoltaics: Research and Applications* 2002; **10**(3): 205–214. DOI: 10.1002/pip. 403.
13. Müllejans H, Zaaiman W, Merli F, Dunlop ED, Ossenbrink HA. Comparison of tracelable calibration methods for primary photovoltaic reference cells. *Progress in Photovoltaics: Research and Application* 2005; **13**(8): 661–671. DOI: 10.1002/pip. 625.
14. Fabero F, Alonso-Abella M, Chenlo F. Influence of irradiance variations on PV systems at different time scales. *Proceedings of the 14th PVSEC*, Barcelone, 1997; 2299–2302.
15. Jardine CN, Conibeer GJ, Lane K. PV-COMPARE: Direct comparison of eleven PV technologies at two locations in Northern and Southern Europe. *Proceedings of the 17th European PVSEC*, Munich, 2001; 724–727.
16. Jardine CN, Lane K. PV-COMPARE: Relative performance of photovoltaic technologies in Northern and Southern Europe. *Proceedings of the PV in Europe Conference*, Rome, 2002; 1057–1060.